Study of Phase Formation Processes in Li₂ZrO₃ Ceramics Obtained by Mechanochemical Synthesis

Maxim V. Zdorovets [1,2,3], **Artem L. Kozlovskiy** [1,4,*], **Baurzhan Abyshev** [2], **Talgat A. Yensepbayev** [4], **Rizahan U. Uzbekgaliyev** [4] and **Dmitriy I. Shlimas** [1,2]

[1] Laboratory of Solid State Physics, The Institute of Nuclear Physics, Almaty 050032, Kazakhstan; mzdorovets@gmail.com (M.V.Z.); shlimas@mail.ru (D.I.S.)

[2] Engineering Profile Laboratory, L.N. Gumilyov Eurasian National University, Nur-Sultan 010008, Kazakhstan; baurzhan.abyshev@gmail.com

[3] Department of Intelligent Information Technologies, Ural Federal University, 620075 Yekaterinburg, Russia

[4] Institute of Geology and Oil and Gas Business, Satbayev University, Almaty 050032, Kazakhstan; t.yensepbayev@satbayev.university (T.A.Y.); r.uzbekgaliyev@satbayev.university (R.U.U.)

[*] Correspondence: kozlovskiy.a@inp.kz; Tel./Fax: +7-702-441-3368

Abstract: The article is dedicated to the study of the phase formation processes in Li₂ZrO₃ ceramics obtained by the method of solid phase synthesis. Interest in these types of ceramics is due to their great potential for use as blanket materials in thermonuclear reactors, as well as being one of the candidates for tritium breeder materials. Analysis of the morphological features of the synthesized ceramics depending on the annealing temperature showed that the average grain size is 90–110 nm; meanwhile the degree of homogeneity is more than 90% according to electronic image data processing results. The temperature dependences of changes in the structural and conducting characteristics, as well as the phase transformation dynamics, have been established. It has been determined that a change in the phase composition by displacing the impurity LiO and ZrO₂ phases results in the compaction of ceramics, as well as a decrease in their porosity. These structural changes are due to the displacement of LiO and ZrO₂ impurity phases from the ceramic structure and their transformation into the Li₂ZrO₃ phase. During research, the following phase transformations that directly depend on the annealing temperature were established: LiO/ZrO₂/Li₂ZrO₃ → LiO/Li₂ZrO₃ → Li₂ZrO₃. During analysis of the obtained current-voltage characteristics, depending on the annealing temperature, it was discovered that the formation of the Li₂ZrO₃ ordered phase in the structure results in a rise in resistance by three orders of magnitude, which indicates the dielectric nature of the ceramics.

Keywords: lithium-containing ceramics; blankets; Li₂ZrO₃; phase transformations; mechanochemical synthesis

1. Introduction

Recently, in the light of global trends in energy development and the search for alternative sources of energy in order to decarbonize the energy sector and the economies of developed countries, more and more attention has been paid to nuclear energy. A great amount of attention in this field is primarily related to the possibility of obtaining a large amount of energy, which can be used not only to meet the needs of large cities and enterprises, but also to produce hydrogen, which will be an alternative energy source in the near future [1–3]. The most promising projects in this direction are high-temperature nuclear reactors as well as thermonuclear reactors, which will allow the accumulation of tritium for further use as an alternative fuel. The processes associated with tritium accumulation are based on its production and accumulation in the blanket material, followed by absorption and desorption of the obtained tritium from the blanket [4,5]. The most common method for producing tritium is nuclear reaction under the influence of thermal neutrons $^6\text{Li} + n \rightarrow\ ^4\text{He} + T + 4,8$ MeV, which allow not only the production of tritium, but also its accumulation [6]. At the same time, according to the concept of the European

development program for thermonuclear technologies, some of perspective materials for the reproduction of tritium are considered lithium-containing ceramics based on lithium metalates Li_2MO_3 (M = Zr, Ti, Hf, Si) [7–10].

Among the variety of lithium-containing ceramics, ceramics based on lithium metazirconates (Li_2ZrO_3), which are considered as the main materials for tritium multiplication in the concept of solid-state blanket materials for thermonuclear or high-temperature nuclear reactors, are of particular interest [11–13]. The most pronounced advantages of this type of ceramics include high compatibility with structural materials and reflector materials, in particular with beryllium, high mechanical and corrosion resistance, and excellent indicators of the release and accumulation of tritium during irradiation. Interest in Li_2ZrO_3 ceramics is also due to their properties, characterized by absence of the possibility of isotopic exchange, which results in a reduction in the absorption of hydrogen on the surface and inside the particles [14,15]. As a result, all of the formed tritium is absorbed on the ceramic surface without hydrogen impurities, which excludes the subsequent separation of tritium and hydrogen.

However, despite great interest in these ceramics, there are many unresolved issues related primarily to size effects and phase composition effects on the properties of ceramics [16,17]. A number of papers have indicated that nanostructured ceramics are of the greatest interest, the small grain size of which increases the specific surface area as well as the porosity of ceramics, which will contribute to the accelerated absorption of tritium on the surface of ceramics. An important factor is the phase composition of ceramics, which can play a significant role in the production and accumulation of tritium. The point is that the presence of impurities or phase inclusions arising during the preparation of ceramics can lead to the formation of metastable states or strongly deformed regions in the structure, the presence of which can negatively affect the stability of ceramics in the future. Today, there are a large number of different methods for obtaining lithium-containing ceramics that allow them to be obtained with various sets of physicochemical and morphological properties [18–21]. One of the promising production methods is the mechanochemical synthesis method combined with thermal annealing of the obtained mixtures after grinding. Using this method, it is possible to obtain powders of different grain sizes, and subsequent thermal treatment allows for the control of the phase composition of ceramics, as well as the annealing impurity inclusions and phases, thereby initiating phase transformation processes. At the same time, an important factor affecting the applicability of these ceramics as blanket materials is the maintenance of a balance between grain morphology and phase composition of ceramics in order to eliminate the negative consequences of impurity inclusions [22–25].

In view of the aforementioned, the objective of this paper is to examine the phase transformation processes in Li_2ZrO_3 ceramics depending on the sintering temperature, and the effect of impurity inclusions on the properties of ceramics. Interest in this study is due to the possibility of developing a method for obtaining Li_2ZrO_3, which can be used later as a blanket material for tritium multiplication.

2. Experimental Part

2.1. Chemical Reagents

To obtain the ceramics, the following chemical reagents were used: $LiClO_4 \cdot 3H_2O$ and ZrO_2 in the form of micron-sized powders. All reagents were acquired from Sigma Aldrich (Saint Louis, MO, USA) with chemical purity of 99.95%.

2.2. Mechanochemical Synthesis

The samples were synthesized using the mechanochemical synthesis method in a PULVERISETTE 6 classic planetary mill (Fritsch, Idar-Oberstein, Germany). For grinding, a tungsten carbide glass was used, the grinding speed was 400 rpm, and the grinding time was 1 h. The ratio of the sample mass to the mass of the balls used for grinding was 1:5, the choice of this mass ratio corresponded to filling the glass with a volume equal to 2/3 of

the total volume. The synthesis of the samples was carried out in two stages. The first stage included weighing the initial powders, followed by grinding them in a planetary mill until a homogeneous powder was obtained. The second stage consisted in annealing the obtained powders in a given temperature range. After sintering, the samples were studied by various research methods.

After the initial powders were suspended at an equal ratio of 1:1, they were placed in a beaker, then milled. After grinding, the resultant mixture was annealed in a muffle furnace at a temperature range of 600 to 1100 °C with isochronous annealing for 5 h. After annealing, the samples were cooled along with the furnace for 24 h, then taken out and subjected to further studies.

2.3. Study of Morphological Features

The morphological features and homogeneity of particle sizes obtained as a result of mechanochemical synthesis were determined by processing electronic images obtained on a Jeol F7500 (Jeol, Tokyo, Japan) scanning electron microscope.

2.4. Study of the Phase Composition and Structural Characteristics

To define the phase composition and structural parameters of the synthesized ceramics, the X-ray phase analysis method was used. The recording of diffraction patterns was implemented on a D8 Advance ECO powder diffractometer (Bruker, Ettlingen, Germany) in the Bregg–Brentano recording geometry in the angular range of $2\theta = 20$–$60°$ with a step of $0.03°$. Phase composition was determined by full-profile analysis of the obtained diffraction patterns with subsequent comparison of intensities and position of the main diffraction reflections with reference values from the PDF-2(2016) database. Refinement of phases was carried out with the matching probability of more than 90% of reference card lines with experimental data. The crystal lattice parameters were specified using the interplanar distance analysis method using the Nelson–Taylor formulas.

2.5. Determination of the Optical and Electrical Properties of Ceramics

The optical properties of the ceramics were defined using the method of processing UV-Vis spectra obtained on a Jena Specord-250 BU UV-Vis spectrometer. The spectra were recorded in the wavelength range of 200–1000 nm with a step of 1 nm. The main purpose of measuring the optical properties was to determine the magnitude of the absorption, as well as the refractive index of the synthesized ceramics, which makes it possible to estimate the density and porosity of the material, as well as the absorbing capacity, knowledge of which will further determine the absorption properties of ceramics in experiments on gas evolution and accumulation of tritium.

The electrical properties were defined by analyzing the cyclic volt-ampere curves obtained in the range of −4 to 4 V, with a step of 0.1 using a PalmSens 3+ (PalmSens BV, Utrecht, The Netherlands) potentiostat.

Conductive properties were determined by the standard four-contact method using copper electrodes, which allow the obtaining of the volt-ampere characteristics of the samples as well as the determining of the resistivity value by calculations. The main purpose of studying these characteristics was to determine the effect of impurity phases and inclusions on the current-voltage characteristics and changes in the resistance of ceramics, as well as to study changes in the conducting characteristics in the case of phase transformations caused by thermal sintering.

3. Results and Discussion

Figure 1 presents the results of morphological studies of synthesized ceramics depending on the sintering temperature. Images were acquired using scanning electron microscopy (SEM).
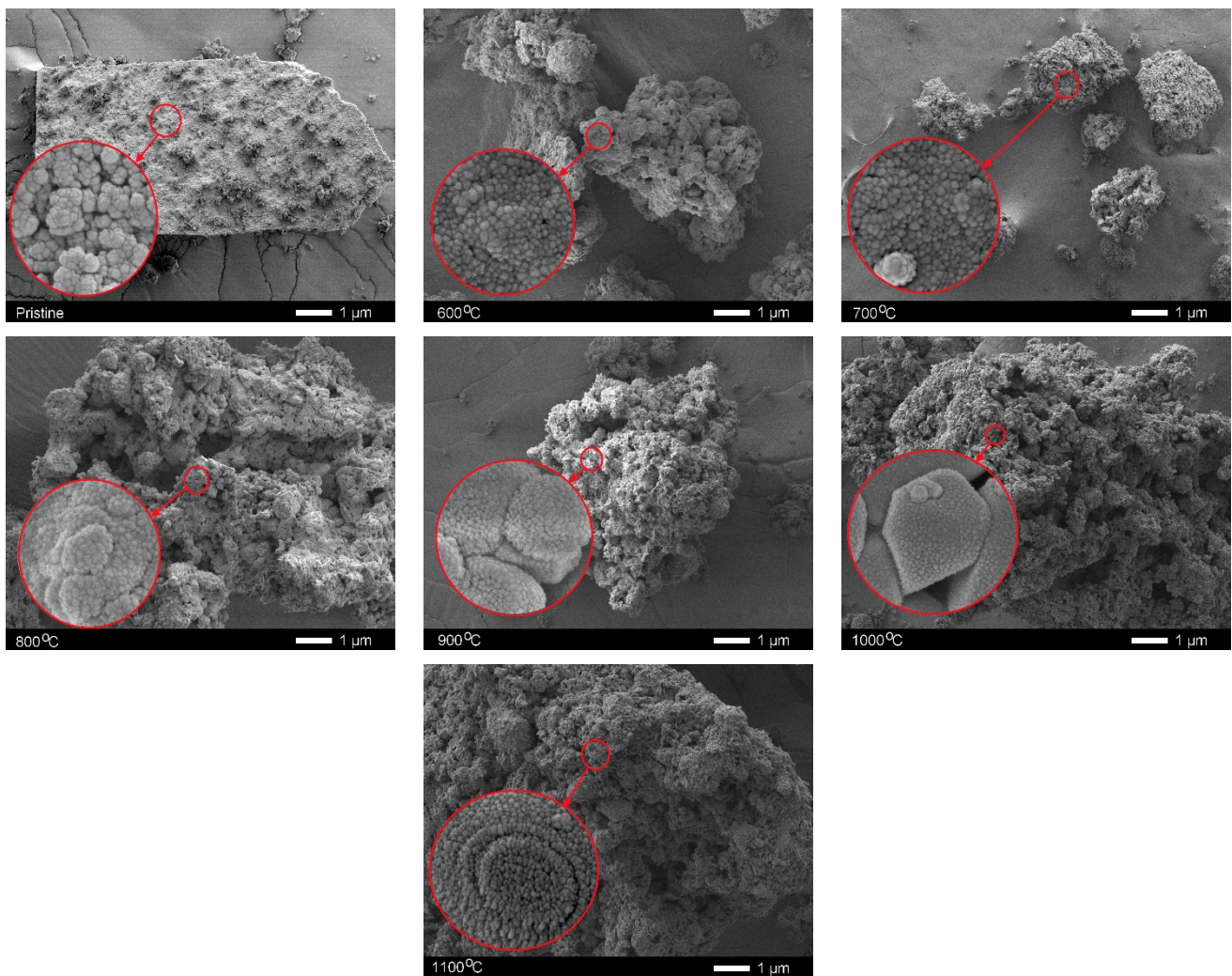
Figure 1. SEM images of synthesized ceramics depending on the annealing temperature.

For comparison, the results of the morphological features of ceramics in the initial state after mechanochemical synthesis are presented. As is evident from the data presented, the ceramics are large agglomerates of various shapes in the reference condition and a detailed analysis of them revealed that they consist of spherical grains, the size of which varies from 150 to 230 nm. For annealed samples, there is a minor decrease in grain size to 90–110 nm, while the degree of homogeneity of grain size increases. A rise in the annealing temperature to 1000 °C resulted in the formation of pyramidal or rhombohedral grains consisting of small particles, which indicates structural ordering and emergence of close-packed particles with low porosity.

Figure 2 presents the results of X-ray phase analysis of the samples under study in relation to the annealing temperature. The general view of the obtained diffraction patterns indicates the polycrystalline structure of ceramics, and the dynamics of the change in shape of the diffraction lines depending upon the annealing temperature characterizes the change in phase composition and structure ordering degree.
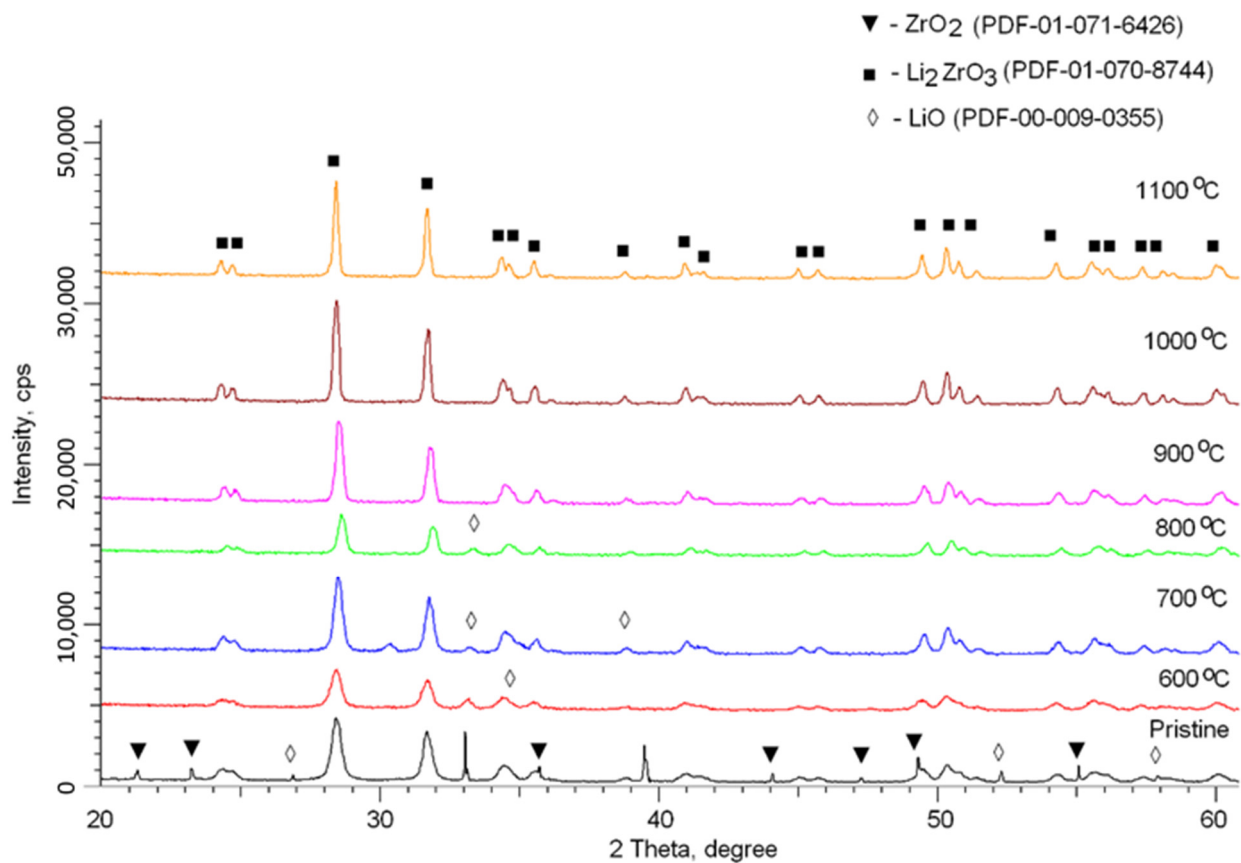
Figure 2. X-ray diffraction patterns of the studied ceramics versus annealing temperature.

According to the assessment of the obtained diffraction pattern of the samples in the reference condition, it was found that the difference in diffraction line shapes, their positions, and their intensities corresponds to the occurrence of several phases in the ceramic structure. Using full-profile analysis, it was revealed that in the initial state the ceramic phase composition is a compound of three phases: the hexagonal LiO phase of the spatial system P-6(174), the orthorhombic ZrO_2 phase of the spatial system Pbcm(57), and the monoclinic Li_2ZrO_3 phase of the spatial system C2/c(15). The presence of impurity LiO and ZrO_2 phases in the structure of the initial ceramics was caused by the phase formation processes resulting from mechanical grinding, which is accompanied by a large number of deformations and distortions of grains, leading to the formation of phases. The distorted asymmetric diffraction maxima shape testifies to a high degree of structural distortions and deformation of the crystal structure of the ceramics in the initial state.

For the annealed samples, according to X-ray diffraction patterns, a rise in the annealing temperature results in a growth in the line shapes symmetry degree, and a decrease in the intensity of diffraction maxima for the impurity LiO and ZrO_2 phases, which indicates their displacement or phase transformation resulting from thermal sintering.

The contribution of different phases was determined using the method for estimating the areas of diffraction lines corresponding to different phases, followed by their calculation using the formula $V_{admixture} = \frac{RI_{phase}}{I_{admixture} + RI_{phase}}$, where I_{phase}—average integrated intensity of the diffraction line main phase, $I_{admixture}$—the average integrated intensity of the additional phase, and $R = 1.45$. Findings of phase composition change dynamics are shown in Figure 3.
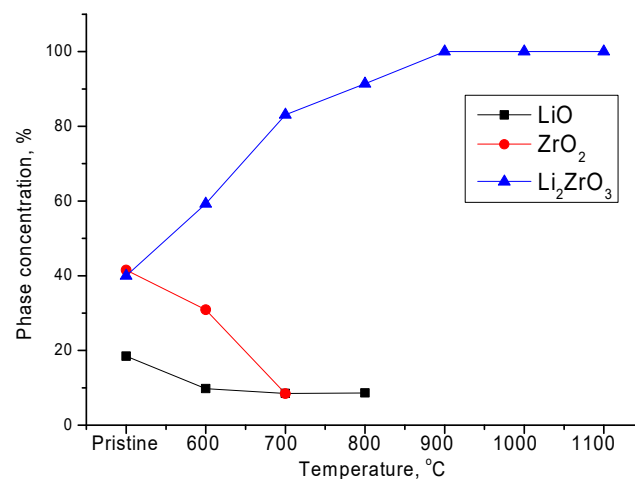
Figure 3. Phase diagram of the studied ceramic samples versus annealing temperature.

The main phase transformations, in relation to the annealing temperature, may be classified in two stages. The first stage is characterized by the displacement of impurity LiO and ZrO_2 phases from the structure of the ceramics, as well as partial ordering of the structure as a result of a change in the phase relation. At an annealing temperature of 800 °C, the displacement or complete transformation of the ZrO_2 phase in the structure of ceramics occurs. The turning point in this case is the temperature of 900 °C, at which the impurity inclusions are completely displaced and the phase formation process ends with the emergence of a stable monoclinic Li_2ZrO_3 phase. A continued growth in the annealing temperature leads only to an increase in the degree of perfection of the crystal structure and ordering of the crystal lattice, as evidenced by the data presented in Table 1. The general scheme of phase transformations in ceramics, in relation to the annealing temperature, may be written in the following form: $LiO/ZrO_2/Li_2ZrO_3 \rightarrow LiO/Li_2ZrO_3 \rightarrow Li_2ZrO_3$.

Table 1. Structural parameter data.

Phase	Lattice Parameter, Å						
	Pristine	600 °C	700 °C	800 °C	900 °C	1000 °C	1100 °C
LiO–Hexagonal P-6(174)	a = 3.14138 c = 7.68150 V = 65.7 Å^3	a = 3.13214 c = 7.64987 V = 64.9 Å^3	a = 3.12047 c = 7.62437 V = 64.3 Å^3	a = 3.11863 c = 7.61092 V = 64.11 Å^3	-	-	-
ZrO_2–Orthorhombic Pbcm(57)	a = 4.98604 b = 5.24120 c = 5.05059 V = 131.9 Å^3	a = 4.98115 b = 5.15456 c = 5.04366 V = 132.1 Å^3	a = 4.97041 b = 5.24529 c = 5.02487 V = 131.1 Å^3	-	-	-	-
Li_2ZrO_3–Monoclinic C2/c(15)	a = 5.40592 b = 8.96082 c = 5.39526 β = 112.37° V = 241.7 Å^3	a = 5.39426 b = 8.95555 c = 5.38786 β = 112.083° V = 241.2 Å^3	a = 5.40801 b = 8.91516 c = 5.37413 β = 111.929° V = 240.4 Å^3	a = 5.39210 b = 8.90292 c = 5.36254 β = 111.907° V = 238.8 Å^3	a = 5.38258 b = 8.88372 c = 5.35308 β = 111710° V = 237.8 Å^3	a = 5.36253 b = 8.86107 c = 5.34153 β = 111.601° V = 235.9 Å^3	a = 5.33835 b = 8.84196 c = 5.32582 β = 111.535° V = 233.8 Å^3

The change in the degree of structural ordering and crystal lattice perfection are also evidenced by results of changes in the ceramic density and the crystal structure integral porosity. The results of changing these values are shown in Figure 4.
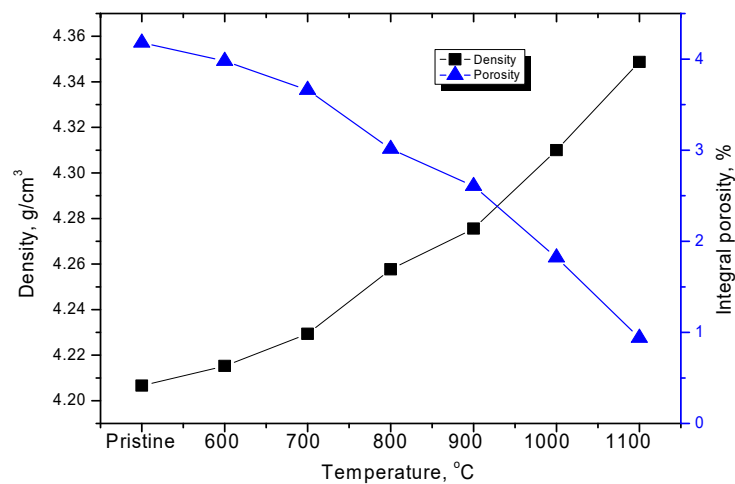
Figure 4. Dynamics of changes in density and porosity of ceramics versus annealing temperature.

The density of ceramics was determined based on changes in structural characteristics, in particular, the crystal lattice volume (V_0) using the formula $p = \frac{1.6602 \sum AZ}{V_0}$, where Z is the number of atoms in a crystal cell and A is the atomic weight of atoms.

The integral porosity, which characterizes the presence of imperfections in the structure and hollow inclusions in the crystal structure, was determined based on changes in ceramic density values in comparison with the reference value.

According to the data obtained, a change in the phase composition followed by the displacement of impurity phases from the structure leads to a growth in the density of ceramics and a decline in the integral porosity value. The largest reduction in the concentration of hollow inclusions was observed at an annealing temperature of 1000–1100 °C, which corresponds to the stage of structural ordering of ceramics, after the completion of the phase formation processes.

Among the most important features of ceramics is their transmittance and absorption capacities, which characterize the optical properties of ceramics, which depend on their structural ordering degree and phase composition. Figure 5 presents the findings of changes in the optical properties of the synthesized ceramics in relation to the annealing temperature. As is evident from data presented, the synthesized ceramics have a fairly good transmittance, while a change in the phase composition results in an insignificant decline in the transmittance, which might be connected with a change in the electron density of the ceramics as a result of the displacement of impurity phases and the ordering of the structure. In the case of absorption capacity, it was revealed that a growth in the degree of structural ordering results in a rise in absorption in the 350–500 nm region, characteristic of the UV and visible light boundary.

Figure 5c reveals the results of changes in the band gap and refractive index, reflecting the optical and electronic properties of ceramics. As is evident from the presented data, a rise in the annealing temperature leading to phase transformations results in a decrease in the refractive index due to the compaction of ceramics and a decrease in porosity. In this case, a change in the phase composition leads to an increase in the band gap, which indicates a change in the electron density of ceramics.

Figure 6 shows the dependences of the cyclic current-voltage characteristics of the studied ceramics versus the annealing temperature.
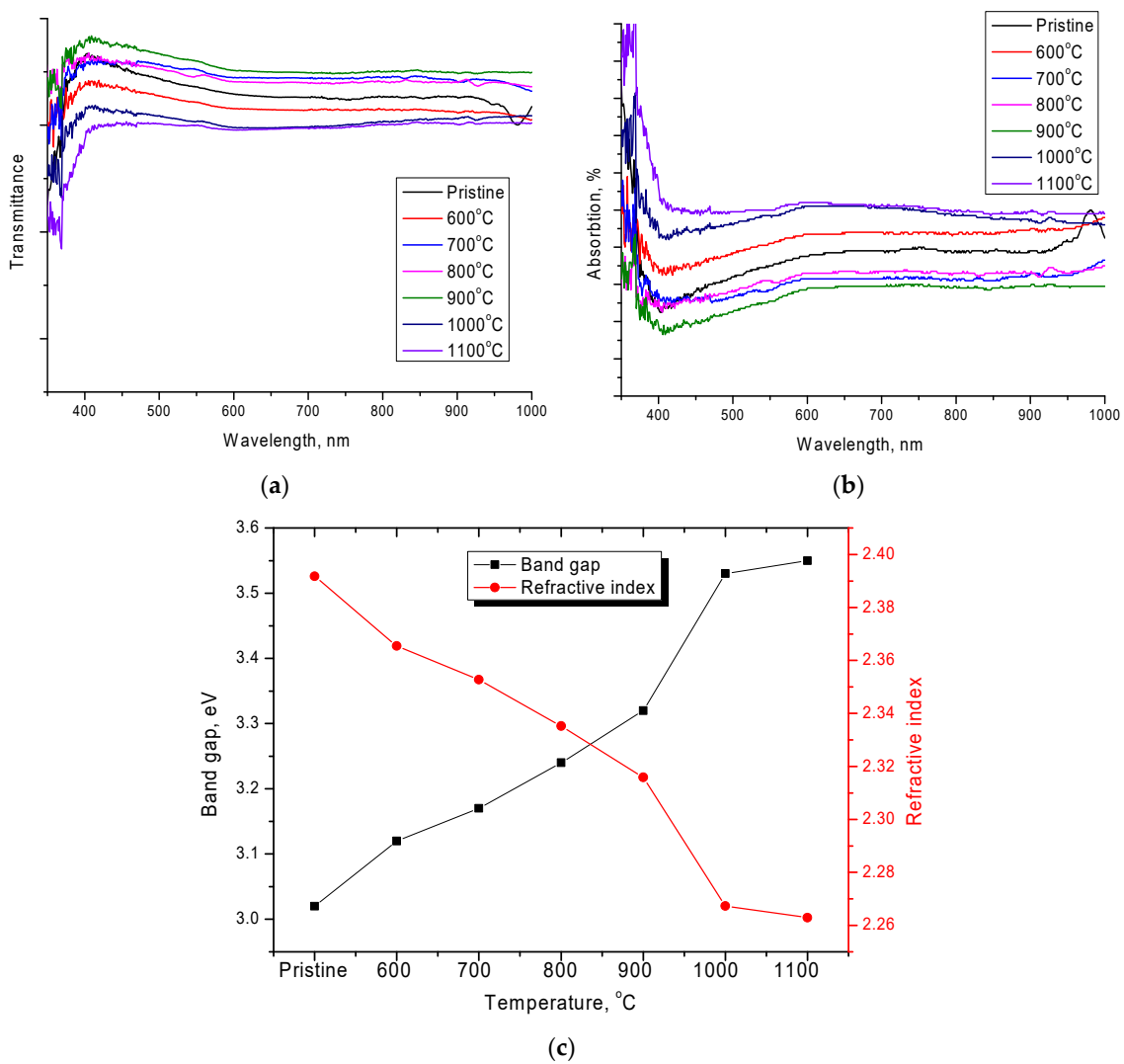
Figure 5. UV-Vis spectra of the studied Li_2ZrO_3 ceramics: (**a**) transmittance; (**b**) absorption; (**c**) results of change in the band gap and refractive index.
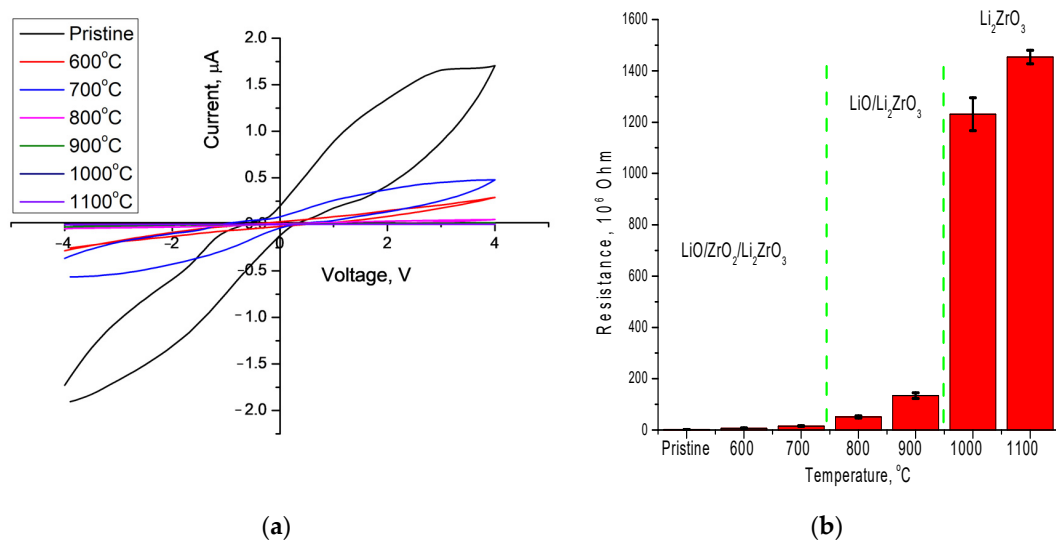

Figure 6. (**a**) IVC graphs of the studied ceramics; (**b**) resistance diagram of the ceramics.

The general view of the loops of current-voltage characteristics for the initial sample indicates the presence of a large number of oxygen vacancies in the structure, which leads to broadening of the loop. This behavior of the loops for the initial sample, as well as for the samples annealed at temperatures of 600–700 °C, is caused by the occurrence of impurity LiO and ZrO_2 phases in the structure, the presence of which determines the presence of free charge carriers, thereby reducing the resistance. A rise in the structural ordering degree and the displacement of impurity inclusions from the structure leads to growth in the resistance and restoration of the dielectric nature of the ceramics.

The difficulties of the applied method include the fact that, at annealing temperatures below 1000 °C, the presence of impurity phases is observed in the structure of ceramics, which lead to the appearance of additional distortions, as well as the appearance of free charge carriers, the presence of which determines the high conductivity of ceramics. An increase in the annealing temperature above 1000 °C leads to the completion of phase transformations with the displacement of impurity phases from the structure, as well as the compaction of ceramics and a decrease in porosity.

4. Conclusions

In conclusion, we can summarize the results of the experimental work. During performed experiments, the dynamics of structural and phase orderings in Li_2ZrO_3 ceramics versus the annealing temperature was established. A two-stage character of phase transformations was established in relation to the annealing temperature, including the displacement of impurity LiO and ZrO_2 phases, followed by structure ordering and a decrease in porosity at temperatures above 900 °C. The general scheme of phase transformations in ceramics is established depending on the annealing temperature, which can be written as $LiO/ZrO_2/Li_2ZrO_3 \rightarrow LiO/Li_2ZrO_3 \rightarrow Li_2ZrO_3$. Analysis of the optical properties of ceramics showed that a change in the phase composition, accompanied by the displacement of impurity phases, leads to an increase in absorption and a change in the transmission of ceramics. During analysis of the obtained current-voltage characteristics depending on the annealing temperature, it was revealed that the formation of the ordered Li_2ZrO_3 phase in the structure results in a rise in resistance by three orders of magnitude, which indicates the dielectric nature of the ceramics.

The practical significance of the work includes the obtained dependencies of phase formation processes in Li_2ZrO_3 ceramics, which make it possible to conclude that the use of the proposed mechanochemical synthesis method with consequential thermal annealing of samples at temperatures of 1000–1100 °C allows for the obtaining of nanostructured single-phase ceramics with a high degree of homogeneity of grain sizes and an ordered crystal structure without impurity inclusions.

Further research within the framework of ongoing work on this topic will be aimed at studying the radiation resistance of Li_2ZrO_3 ceramics and determining the kinetics of radiation embrittlement and swelling of ceramics in relation to the type of radiation exposure.

Author Contributions: Conceptualization, M.V.Z., B.A. and A.L.K.; methodology, B.A., T.A.Y. and A.L.K.; formal analysis, R.U.U., D.I.S. and M.V.Z.; investigation, B.A., A.L.K. and M.V.Z.; resources, M.V.Z.; writing—original draft preparation, review, and editing, B.A., M.V.Z. and A.L.K.; visualization, M.V.Z.; supervision, M.V.Z. All authors have read and agreed to the published version of the manuscript.

Institutional Review Board Statement: Not applicable.

Informed Consent Statement: Informed consent was obtained from all individual participants included in the study.

Data Availability Statement: Not applicable.

Conflicts of Interest: The authors declare no conflict of interest.

Ethical Approval: This chapter does not contain any studies with human participants or animals performed by any of the authors.

References

1. Şahin, S.; Şahin, H.M.; Şahiner, H.; Tunç, G. Study on the fusion reactor performance with different materials and nuclear waste actinides. *Int. J. Energy Res.* **2021**, *45*, 11759–11774. [CrossRef]
2. Ling, Q.; Wang, G. A research and development review of water-cooled breeding blanket for fusion reactors. *Ann. Nucl. Energy* **2020**, *145*, 107541. [CrossRef]
3. Swami, H.L.; Sharma, D.; Mistry, A.N.; Danani, C.; Chaudhuri, P.; Srinivasan, R. Helium cooled dual breeder blanket–preliminary design analyses of a candidate breeding blanket concept for near term Indian DEMO fusion reactor. *Int. J. Energy Res.* **2021**, *45*, 11735–11744. [CrossRef]
4. Cui, S.; Zhang, D.; Lang, Y.; Jiang, X.; Tian, W.; Su, G.; Cao, Q.; Wu, X.; Zhao, F.; Li, J. A new method for improving the tritium breeding and releasing performance of China Fusion Engineering Test Reactor phase II helium-cooled ceramic breeder blan-ket. *Int. J. Energy Res.* **2020**, *44*, 5977–5989. [CrossRef]
5. Salvatores, M.; Orsitto, F.; Carta, M.; Burgio, N.; Fabrizio, V.; Falconi, L.; Pal-omba, M.; Panza, F. An approach to the experimental validation of the fission multi-plying blanket of hybrid fusion fission systems. *Ann. Nucl. Energy* **2021**, *157*, 108055. [CrossRef]
6. Mandal, R.; Vijayaraghavan, P.R.; Bhoraskar, V.N.; Sengupta, D. Neutron depth profiling using the reactions 10 B (n, α) 7 Li and 6 Li (n, α) 3 H induced by ther-mal neutrons. *J. Radioanal. Nucl. Chem.* **2020**, *325*, 983–987. [CrossRef]
7. Lulewicz, J.; Roux, N.; Piazza, G.; Reimann, J.; van der Laan, J. Behaviour of Li_2ZrO_3 and Li_2TiO_3 pebbles relevant to their utilization as ceramic breeder for the HCPB blanket. *J. Nucl. Mater.* **2000**, *283*, 1361–1365. [CrossRef]
8. Lulewicz, J.D.; Roux, N.; Piazza, G.; Reimann, J.; Van der Laan, J. Isotope ex-change capacity on Li_4SiO_4 and comparison of tritium inventory in various solid breeder blankets. *J. Nucl. Sci. Technol.* **2001**, *38*, 944–951.
9. Kanazawa, T.; Nishikawa, M.; Yamasaki, H.; Katayama, K.; Kashimura, H.; Hanada, T.; Fukada, S. Study on Tritium Release Behavior from Li_2ZrO_3. *Fusion Sci. Technol.* **2011**, *60*, 1167–1170. [CrossRef]
10. Kinjyoa, T.; Nishikawaa, M.; Katayamaa, K.; Tanifujib, T.; Enoedac, M.; Beloglazovd, S. Release Behavior of Bred Tritium from Irradiated Li_4SiO_4. *Fusion Sci. Technol.* **2005**, *48*, 646–649. [CrossRef]
11. Li, K.; Yang, W.; Wang, W.H.; Li, Y.T. Tritium adsorption in the lithium va-cancy of Li_2ZrO_3: A first principles study. *Int. J. Mod. Phys. C* **2018**, *29*, 1850103. [CrossRef]
12. Paudel, H.P.; Duan, Y. A First-Principles Density Function Theory Study of Tritium Diffusion in Li_2ZrO_3: Application for Producing Tritium. *J. Phys. Chem. C* **2018**, *122*, 28447–28459. [CrossRef]
13. Rex, K.A.; Iyngaran, P.; Kuganathan, N.; Chroneos, A. Defect Properties and Lithium Incorporation in Li_2ZrO_3. *Energies* **2021**, *14*, 3963. [CrossRef]
14. Murata, I.; Nishio, T.; Kokooo Kondo, T.; Takagi, H.; Nakano, D.; Takahashi, A.; Maekawa, F.; Ikeda, Y.; Takeuchi, H. Bench-mark experiment on $LiAlO_2$, Li_2TiO_3 and Li_2ZrO_3 assemblies with D–T neutrons–leakage neutron spectrum measurement. *Fusion Eng. Des.* **2000**, *51*, 821–827. [CrossRef]
15. Rao, G.J.; Mazumder, R.; Bhattacharyya, S.; Chaudhuri, P. Fabrication of Li_4SiO_4-Li_2ZrO_3 composite pebbles using extrusion and spherodization technique with improved crush load and moisture stability. *J. Nucl. Mater.* **2019**, *514*, 321–333. [CrossRef]
16. Zeng, Y.; Chen, R.; Yang, M.; Wang, H.; Guo, H.; Shi, Y.; Huang, Z.; Qi, J.; Shi, Q.; Lu, T. Fast fabrication of high quality Li_2TiO_3–Li_4SiO_4 biphasic ceramic pebbles by microwave sintering: In comparison with conventional sintering. *Ceram. Int.* **2019**, *45*, 19022–19026. [CrossRef]
17. Lu, W.; Wang, J.; Pu, W.; Li, K.; Ma, S.; Wang, W. Sol-gel synthesis of lithium metatitanate as tritium breeding material under different sintering conditions. *J. Nucl. Mater.* **2018**, *502*, 349–355. [CrossRef]
18. Shlimas, D.I.; Zdorovets, M.V.; Kozlovskiy, A.L. Synthesis and resistance to helium swelling of Li_2TiO_3 ceramics. *J. Mater. Sci. Mater. Electron.* **2020**, *31*, 12903–12912. [CrossRef]
19. Gupta, C.K. *Materials in Nuclear Energy Applications*; CRC Press: Boca Raton, FL, USA, 2018; Volume I.
20. Zdorovets, M.V.; Kozlovskiy, A.L. The effect of lithium doping on the ferroelectric properties of LST ceramics. *Ceram. Int.* **2020**, *46*, 14548–14557. [CrossRef]
21. Hernández, F.A.; Pereslavtsev, P. First principles review of options for tritium breeder and neutron multiplier materials for breeding blankets in fusion reactors. *Fusion Eng. Des.* **2018**, *137*, 243–256. [CrossRef]
22. Chen, R.; Shi, Q.; Yang, M.; Shi, Y.; Wang, H.; Dang, C.; Qi, J.; Liao, Z.; Lu, T. Microstructure and phase evolution of Li_4TiO_4 ceramics pebbles prepared from a nanostructured precursor powder synthesized by hydrothermal method. *J. Nucl. Mater.* **2018**, *508*, 434–439. [CrossRef]
23. Davies, A.W.; Murphy, S.T. Fundamental properties of octalithium plumbate ceramic breeder material. *J. Nucl. Mater.* **2021**, *552*, 152982. [CrossRef]
24. Zhou, Q.; Oya, Y.; Chikada, T.; Zhang, W.; Xue, L.; Yan, Y. Preparation of Li_2TiO_3 by hydrothermal synthesis and its structure evolution under high energy Ar^+ irradiation. *J. Eur. Ceram. Soc.* **2017**, *37*, 4955–4961. [CrossRef]
25. Shlimas, D.I.; Zdorovets, M.V.; Kozlovskiy, A.L. Study of Corrosion Re-sistance and Degradation Mechanisms in $LiTiO_2$-Li_2TiO_3 Ceramic. *Crystals* **2021**, *11*, 753. [CrossRef]